

Field Oriented Control For Three Phase Induction Motor Based On Full Neural Estimator And Controller

Fadhil A. Hassan*

Received on: 3/3/2010

Accepted on: 3/6/2010

Abstract

Closed loop speed control for an IM is somewhat complex strategy, the complexity is gradually increases according to the demand performance degree. There are many types of control strategies: scalar, direct torque, adaptive, sensor less, and vector or Field Oriented Control (FOC). This paper proposes the FOC strategy in details. Rotor flux, unit vector, and electromagnetic torque estimation are considered by using Digital Signal Processing (DSP). Artificial Neural Network (ANN) becomes a powerful tool for control nonlinear system in present time. This study proposes the using of ANN in stead of DSP to estimate the flux, unit vector, and electromagnetic torque to reduce the hardware complexity and the Electromagnetic Interference (EMI) effect. Also, it proposes the PI neural-based controller. The overall system simulation for both DSP and ANN are proposed. The performances of both systems are investigated, which give in DSP: rise time 0.24 sec, settling time 0.29 sec, overshoot 5%, steady state error 0.5%. Whereas, in ANN: rise time 0.18, settling time 0.19 sec, overshoot 1%, steady state error 0.2%.

Keywords: Field Oriented Control, DSP Estimation, Neural Estimation, PI Neural-Based Controller.

السيطرة بطريقة تحييد المجال على المحرك الحثي الثلاثي الطور باستخدام عصبي كامل في المخمن والمسيطر

الخلاصة

تعتبر السيطرة على سرعة المحرك الحثي باستخدام الحلقة المغلقة معقدة نوعاً ما، ويزداد التعقيد وفقاً لدرجة الأداء المطلوبة. هناك عدة أنواع من استراتيجيات السيطرة: المقياسي، العزم المباشر، المتكيف، والمتجه أو تحييد المجال. تقدم هذه الورقة استراتيجيات تحييد المجال بالتفصيل. حيث تم تخمين متجه المجال ومتجه الوحدة والعزم الكهرومغناطيسي باستخدام معالجة الإشارات الرقمية. أصبحت الشبكات العصبية الاصطناعية أداة قوية في السيطرة على المنظومات اللاخطية في الوقت الحاضر. تقدم هذه الدراسة استخدام الشبكات العصبية بدلاً عن المعالجة الرقمية في تخمين متجه المجال ومتجه الوحدة والعزم الكهرومغناطيسي للتقليل من تعقيد الدوائر الألكترونية وتأثير التداخلات الكهرومغناطيسية عليها، كما وتقدم المسيطر التناسقي التكاملي باستخدام الشبكات العصبية. وتم تقديم المحاكاة الكاملة لكلا النظامين (المعالج الرقمي و الشبكة العصبية). كما وتم أنتقاء أداء النظامين حيث كان الأداء في نظام المعالج الرقمي: (زمن الأرتفاع 0.24 ثانية، زمن الوضع 0.29 ثانية، والتجاوز 5 %، الخطأ في حالة الأستقرار 0.5 %). في حين كان الأداء في الشبكة العصبية: (زمن الأرتفاع 0.18 ثانية، زمن الوضع 0.19 ثانية، والتجاوز 1 %، الخطأ في حالة الأستقرار 0.2 %).

1. Introduction:

Open loop Variable Voltage Variable Frequency (VVVF) control of an induction motor is by far the most popular method, because of its simplicity, and these types of motors are widely used in industrial applications. Traditionally, the Volt/Hz is controlled by means of D.C-A.C pulse width modulation inverter in order to maintain the air-gap flux approximately at its rated value, this type of control called "scalar control". Unfortunately, scalar control is somewhat simple to implement, but the inherent coupling effect for both torque and flux are functions of voltage or current and frequency (i.e. during volt/Hz variation both torque and flux be varied too), which gives sluggish response and the system is easily prone to instability because of high order system effect[1].

This problem can be solved by vector or field-oriented control, which invented at 1970s, and the demonstration that; an induction motor can be controlled like a separately excited D.C. motor, brought a renaissance in the high performance control of A.C. drives, vector control is also known as decoupling, orthogonal, or trans-vector control. The principle of this method is to rotate the direct axis always in the same direction of the rotor pole axis, or by aligned the rotor flux vector $\overline{\psi}_r$ on the d-axis. This can be done by estimating the exact unit vector ($\cos\theta_e$ and $\sin\theta_e$). In this way it's essential to estimate the flux vector $\overline{\psi}_r$ and the unit vector by using complex digital signal

processing (DSP) and microcomputer analysis[1, 2].

Nowadays, the Artificial Intelligent System (AIS) has penetrated deeply into electrical engineering field and their applications in power electronics and motion control appears very promising [1, 3]. The artificial neural system is one of the most powerful intelligent system with improved design and performance features, which can be implemented in this paper to estimate the flux vector $\overline{\psi}_r$, the unit vector ($\cos\theta_e$ and $\sin\theta_e$), and the electromagnetic torque T_e instead of using the complex microprocessor DSP analysis.

2. Brief Review:

Before entering deeply in field-oriented control, some principles of A.C. drives and system stages must be briefly reviewed to understand system operation. The overall system is consisting of three main stages as shown in figure (1):

- Voltage-fed Sinusoidal Pulse Width Modulation (SPWM) inverter.
- Three phase induction motor.
- Controller.

The last one will be discussed in details later.

2.1 Constant Volt/Hz Control:

The characteristics of 3-phase induction motor have different forms as the variation of input voltage and frequency. The operation characteristics can be divided into three regions [1, 4]:

- i- Constant torque region; where the volt/Hz is kept constant to maintain flux and pull-out torque at their maximum limits.
- ii- Constant power region 1; where the stator voltage reaches rated

value and the frequency increased beyond synchronous frequency. The air-gap flux decreases but the stator current maintained constant by increasing the slip.

iii-Constant region 2; where the torque is inversely proportion with square of speed, because of both of current and flux reduce with speed increasing.

The last two regions are known as field weakening region [1].

2.2 Voltage-Fed Inverter:

2.2.1 Sinusoidal PWM Inverter:

The pulse width modulation techniques have wide simple and complex types, the Sinusoidal Pulse Width Modulation (SPWM) is the most popular used method of A.C. drives, but it's not the efficient method [1, 5]. Voltage source inverter (VSI) should have a stiff source at the input [1], that is, its Thevenin impedance ideally is zero. Thus, a large capacitor can be connected at the input if the voltage source is not stiff. A practical (VSI) consist of power bridge devices with three output legs, each consist of two power switches and two freewheeling diodes, the inverter is supplied from D.C. voltage source via LC or C filter. In sinusoidal PWM the three output legs considered as three independent push-pull amplifiers [5]. The gating signals of each push-pull stage generated by comparing a constant level triangle signal of frequency (f_c) called "carrier signal", with 3-phase sinusoidal signals of frequency (f_m) called "reference signals", which has variable amplitude to get the desired output voltage, this comparison leads to generate a sequence of variable width pulses used to gating each switch in the push-pull stage. Figure

(2) illustrates the principles of SPWM; gating signals, phase voltage. The output phase voltage:

V_{ao} = is the output phase voltage measured to the center of the input D.C. voltage.

V_{an} = is the output phase voltage measured to isolated neutral of three-phase load such as induction motor.

Where:

$$\begin{bmatrix} V_{an} \\ V_{bn} \\ V_{cn} \end{bmatrix} = \frac{1}{3} \begin{bmatrix} 2 & -1 & -1 \\ -1 & 2 & -1 \\ -1 & -1 & 2 \end{bmatrix} \begin{bmatrix} V_{ao} \\ V_{bo} \\ V_{co} \end{bmatrix} \dots\dots (1)$$

$$V_{ao} = 0.5mV_d \sin(\omega t) + \text{high-frequency} (M \omega_c \pm N\omega) [1] \dots\dots (2)$$

Where: ω = fundamental frequency; ω_c =carrier frequency; M and N are integers and M+N =odd, m=modulation index is defined as [1, 5]:

$$m = \frac{V_p}{V_T} \dots\dots(3)$$

Where: V_p = peak of modulating signal, V_T = peak of triangle signal. At m= 1, the maximum value of fundamental peak = 0.5 V_d which is 78.54% of the peak fundamental voltage of the square-wave (2 V_d/π) which called the linear modulation region. To further increase the amplitude of the output voltage, the amplitude of the modulating signals exceeds the amplitude of the carrier signal which leads to enter into quasi-PWM region called "over modulating region" causing increase in the low order harmonics. Further increasing modulation index tends to obtain

square wave at maximum possible output fundamental ($2V_d/\pi$) [1, 5].

2.2.2 SPWM Inverter Simulation:

By using MATLAB/SIMULINK PROGRAM, the SPWM inverter can be simulated, firstly generation of the carrier triangle signal and the three modulating signals by using internal timer and the rated frequency (50 Hz) to obtain the angular speed ($\omega_e t$), then multiplying the angular speed and the amplitude of the signal by the frequency command (f_{com}^*) and voltage command (V_{com}^*) respectively. Secondly, compared the two signal sets to generate the switching signals of three switches used as three push-pull devices. The output of the switches gives (V_{ao}, V_{bo}, V_{co}) then the three phase to load neutral (V_{an}, V_{bn}, V_{cn}) can be achieved by implementing equation (1). Figure (3) illustrated the complete simulation of SPWM inverter, and the output phase voltage can be shown in figure (4).

2.3 Modeling and Simulation of Three Phase I.M.:

The mathematical representation of an induction motor can be looked on as transformer with moving secondary winding, where the coupling coefficients between the stator and rotor phases change continuously with the change of rotor position [1, 5]. The machine model can be described by differential equation with time varying mutual inductances, but such model tends to be very complex. Therefore, axis transformation is applied to transfer the three phase parameters (voltage, current and flux) to two-axis frame called (dq-axis stationary frame or

park transformation). Park transformation is applied to refer the stator variables to a synchronously rotating reference frame fixed in the rotor, by such transformation the stator and rotor parameters rotate in synchronous speed and all simulated variables in the stationary frame appear as d.c. quantities in the synchronously rotating reference frame [1, 5].

The per-phase equivalent circuit diagrams of an I.M. in two-axis synchronously rotating reference frame are illustrated in figure (5). From the circuit diagram the following equations can be written [1]:

- Stator equation:

$$V_{qs}^e = R_s i_{qs}^e + \frac{d\Psi_{qs}}{dt} + w_e \Psi_{ds} \dots\dots(4)$$

$$V_{ds}^e = R_s i_{ds}^e + \frac{d\Psi_{ds}}{dt} - w_e \Psi_{qs} \dots\dots\dots(5)$$

- Rotor equation:

$$V_{qr}^e = R_r i_{qr}^e + \frac{d\Psi_{qr}}{dt} + (w_e - w_r) \Psi_{dr} \dots\dots(6)$$

$$V_{dr}^e = R_r i_{dr}^e + \frac{d\Psi_{dr}}{dt} - (w_e - w_r) \Psi_{qr} \dots\dots(7)$$

Where: the superscript notation "e" referred to the synchronously rotating reference frame quantities.

It's obviously that in squirrel cage I.M $V_{dr}=0$, then the pervious equation can be rewritten:

$$\frac{d\Psi_{qs}^e}{dt} = V_{qs}^e - R_s i_{qs}^e - w_e \Psi_{ds}^e \dots(8)$$

$$i_{qs}^e = \frac{\Psi_{qs}^e - \Psi_{dm}^e}{L_s} \dots(16)$$

$$\frac{d\Psi_{ds}^e}{dt} = V_{ds}^e - R_s i_{ds}^e + w_e \Psi_{qs}^e \dots(9)$$

The air gap flux:

$$\frac{d\Psi_{qr}^e}{dt} = -R_r i_{qr}^e - (w_e - w_r) \Psi_{dr}^e \dots(10)$$

$$\Psi_{qm}^e = \frac{L_{m1}}{L_s} \Psi_{qs}^e + \frac{L_{m1}}{L_r} \Psi_{qr}^e \dots(17)$$

$$\frac{d\Psi_{dr}^e}{dt} = -R_r i_{dr}^e + (w_e - w_r) \Psi_{qr}^e \dots(11)$$

$$\Psi_{dm}^e = \frac{L_{m1}}{L_s} \Psi_{ds}^e + \frac{L_{m1}}{L_r} \Psi_{dr}^e \dots(18)$$

The development torque by interaction of air gap flux and rotor current can be found as:

$$T_e = (3/2)(P/2) \overline{\Psi_m^e} \overline{X I_r^e} \dots(12)$$

By resolving the variables into d-q^e components:

$$T_e = (3/2)(P/2) (\Psi_{ds}^e i_{qs}^e - \Psi_{qs}^e i_{ds}^e) \dots(13)$$

The dynamic torque equation of the rotor:

$$T_e = T_L + \left(\frac{2}{P}\right) J \frac{dw_r}{dt} \dots(14)$$

Where: w_r = is the rotor speed; P: no. of poles; J= rotor inertia; T_L= load torque.

$$i_{ds}^e = \frac{\Psi_{ds}^e - \Psi_{qm}^e}{L_s} \dots(15)$$

The stator current can be found by:

Where:

$$L_{m1} = \frac{1}{\left(\frac{1}{L_m} + \frac{1}{L_s} + \frac{1}{L_r}\right)} \dots(19)$$

From the previous equations the dynamic model of an induction motor is simulated as shown in figure (6).

3. A.C Drive Control Strategies:

To perform the desired load task, a close loop control system must be implemented. There are many types of controller, were built and employed according to specific strategies and the desired performance level. The most popular used strategies are [1, 2]:

3.1 Scalar Control:

It's the simplest control method, easy to implement, and have been widely used in industry. As the name indicates, is due to the magnitude variation of the control variables only, and disregards the coupling effect of the machine.

3.2 Direct Torque Control:

It's complex than scalar control, in which the errors between the reference and the estimated values of torque and flux are directly control

the inverter states in order to reduce the torque and flux errors.

3.3 Adaptive Control:

It is more complex than previous types, which deal with variable mechanical parameters load nature. Such controller requires adaptation or tuning of controller parameters in real time, depending on the plant parameter variation and load torque disturbance.

3.4 Sensors Less Control:

Ongoing researches have concentrating on the eliminating of the speed sensor at the machine shaft without deteriorating the dynamic performance of the drive control system. Speed estimation is an issue of particular interest with such controllers.

3.5 Vector or Field-Oriented Control:

Vector or Field-Oriented Control (FOC), allows a squirrel-cage induction motor to be driven with high dynamic performance. It transforms the dynamic structure of the A.C motor into that of separately excited D.C motor [1, 2]. For D.C motor, the field flux is proportional to the field current, if the field assumed to be constant and independent of armature current, the armature current provides direct control torque, so that:

$$T_e \propto I_f * I_a \quad \dots(20)$$

With the induction motor transformed to d-q plane, it looks like a separately excited D.C motor. The (FOC) technique decouples the two components of stator current; one providing the air-gap flux, and the other producing the torque. These current components provide independent control of flux and torque and the characteristic is linear

[1, 2]. These components are transferred back to the stator frame before feeding back to the rotor. The two components are d-axis $i_{d_s}^*$ analogues to field current I_f , and q-axis $i_{q_s}^*$ is analogues to armature current I_a of the separately excited D.C motor [1, 2]. This strategy can be implemented by align the rotor flux vector along the d-axis of the stationary frame as shown by the phasor diagram in figure (7). The fundamentals of vector control implementation can be explained in figure (8), where the motor model is presented in a synchronously rotating reference frame, the voltage-fed SPWM inverter produces three-phase voltages (v_a, v_b, v_c) according to the reference command voltages (v_a^*, v_b^*, v_c^*) the flux component of stator current ($i_{d_s}^*$) and the torque component of the stator current ($i_{q_s}^*$) is used as a control signals to the system, which are inversely transformed to three-phase reference currents (i_a^*, i_b^*, i_c^*), and then transferred to three-phase voltages (v_a^*, v_b^*, v_c^*) through (PI) controller [1, 2]. The vector control can be implemented by either direct or indirect method, these methods are different essentially by how the unit vector ($\cos\theta_e$ and $\sin\theta_e$) is estimated for the controller.

4. Flux Vector Estimation:

There are two commonly methods of flux estimation; voltage model, and current model. The first one has strong performance in high speed regions but not in low speeds. Whereas, the second method has an accepted performance in both low and high speeds [1].

The current model depends on the main rotor equations in the two axes stationary frame d-q^s, superscript "s" referred to stationary frame quantities:

$$R_r i_{qr}^s + \frac{d\Psi_{qr}^s}{dt} - \omega_r \Psi_{dr}^s = 0 \quad \dots\dots\dots(21)$$

$$R_r i_{dr}^s + \frac{d\Psi_{dr}^s}{dt} + \omega_r \Psi_{qr}^s = 0 \quad \dots\dots\dots(22)$$

Adding terms $(L_m R_r / L_r) i_{ds}^s$ and $(L_m R_r / L_r) i_{qs}^s$ and simplifying, get:

$$\Psi_{qr}^s = \int \left[\frac{L_m}{T_r} i_{qr}^s + \omega_r \Psi_{dr}^s - \frac{\Psi_{dr}^s}{T_r} \right] dt \quad (23)$$

$$\Psi_{dr}^s = \int \left[\frac{L_m}{T_r} i_{dr}^s - \omega_r \Psi_{qr}^s - \frac{\Psi_{qr}^s}{T_r} \right] dt \quad (24)$$

Where: $T_r = \frac{L_r}{R_r}$ is the rotor time constant.

Equations (23 & 24) give rotor fluxes as a function of stator currents and speed. Therefore, knowing these signals, the rotor flux and corresponding unit vector ($\cos\theta_s$ and $\sin\theta_s$) can be estimated by means of DSP microprocessor to implement the following equations [1, 2]:

$$\left. \begin{aligned} \overline{\Psi}_r &= \sqrt{\Psi_{qr}^2 + \Psi_{dr}^2} \\ \Psi_{qr}^s &= \overline{\Psi}_r \sin\theta_s \\ \Psi_{dr}^s &= \overline{\Psi}_r \cos\theta_s \end{aligned} \right\} (25)$$

Or: $\sin\theta_s = \frac{\Psi_{qr}^s}{\overline{\Psi}_r}$
 $\cos\theta_s = \frac{\Psi_{dr}^s}{\overline{\Psi}_r}$

Flux estimation by the current model requires a speed encoder, but the advantage is that the drive operation can be extended down to

low and zero speed. It's important to mention, that the input signals to the estimator (i_{qs}^s and i_{ds}^s) must be filtered by a low pass filter stage. The simulation of the current model estimator can be shown in figure (9).

5. DSP Field-Oriented Control Simulation:

As mentioned before, equations (25) implemented by means of DSP microprocessor to estimate the rotor flux $\overline{\Psi}_r$ and the unit vector ($\cos\theta_s$ and $\sin\theta_s$). Then two reference commands are obtained; first the torque command i_{qr}^* , and second the flux command i_{ds}^* , which are D.C values in synchronously rotating frame [1, 2]. These two setting commands are compared with the actual currents i_{qs}^s and i_{ds}^s , the error signals of the two components are converted to voltage reference signals v_{qr}^* and v_{ds}^* by means of two PI controllers, which are converted to three phase reference voltages (v_{as}^* , v_{bs}^* , v_{cs}^*) to drive the SPWM inverter at desired voltage and frequency. The flux command i_{ds}^* obtained from PI flux control loop for precision control of flux, and the torque command i_{qr}^* generated from the speed control loop. The overall close loop simulation of DSP- estimator with PI-controller field oriented speed control is illustrated in figure (10). The flux command $\overline{\Psi}_r^*$ collected with the speed command ω_r^* the lockup table to program the flux during field weakening regions. The operation performance of the motor under different speed steps is shown in figure (11).

6. Artificial Neural Networks:

Nowadays, we have seen extensive researches and developments effort to use the intelligent system in many industrial applications, because of its strong features like: learning ability, massive parallelism, fast adaptation, inherent approximation capability, and high degree of tolerance [6, 7]. Neural Network Controller (NNC) was effectively introduced to improve the performance of nonlinear system, which are a powerful tools used to predict the optimum performance for both identification and control system. The universal approximation capabilities of multi-layer perceptron make it popular choice for modeling nonlinear systems and for implementing general-purpose controllers. The neural network is an intelligent system which could be learned or trained using an actual existing input and output table, learning or training can be achieved in real-time or off-time operation [1, 7].

Thus, these features can be employed in this work to estimate the amount of the rotor flux vector $\overline{\Psi}_r$ and the unit vector $(\cos\theta_s$ and $\sin\theta_s)$ instead of using DSP microprocessor, which reduce the complexity of the hardware, and reduce the Electro Magnetic Interference EMI in the microprocessor performance. Also, a neural-based PI controller can be

implemented instead of hardware PI controller.

6.1 Design of Neural Network Estimator:

A neural network of four input neurons $(i_{qs}^s, i_{ds}^s, \Psi_{qr}^s, \Psi_{dr}^s)$ and four output neurons $(\cos\theta_s, \sin\theta_s, T_e, \Psi_r)$ with 20 hidden layers was trained to achieve the desired output of the estimator. It's important to mention here, that is, traditionally a large number of input and output data of different speed conditions are used to training the neural network, but in this work a single unit step signal with rise and fall-edge is used to training the neural network, which gives an excellent performance in different speed conditions. The accuracy performance of the neural network can be shown in figure (12). And the neural network estimator simulation is shown in figure (13).

6.2 Design of Neural-based PI Controller:

A single neural network has two inputs and outputs neurons with four hidden layers are used to achieve the desired control signal in both of torque and flux component PI controllers. Also, as in the neural estimator, the training process was done by using a single unit step signal with rise and fall-edge. The simulation of the neural-based PI controller is shown in figure (14).

The overall simulation of FOC system with neural estimator and controller is shown in figure (15). The motor performance for different speed steps is shown in figure (16),

and the rotor speed accuracy performance for gradually increasing of command speed from 0-140% of rated speed with estimated unit vector are shown in figure (17).

7. Conclusions

8. In this work the issue of FOC strategy and its performance of an induction motor were analyzed for both of DSP estimator PI controller and neural estimator-controller. The obtained conclusion can be summarized as following:

1. Obviously, FOC is a powerful complex controller according to high performance demand, which give strong performance in different speed steps, under full-load condition in both constant torque and field weakening operation regions.

2. The DSP-estimator PI-controller gives an excellent performance as shown in figure (11), in which the rise time to achieve the command speed is approximately 0.24 sec, the overshoot response is less than 5%, settling time about 0.29 sec and the steady state error is less than 0.5%.

3. The implementation to Neural estimator and controller is not reduce the hardware complexity only, but it improves the system performance, which gives: rise time 0.18 sec, overshoot less than 1%, settling time 0.19 sec, and steady state error less than 0.2% as shown in figure (16).

4. The estimation unit vector and electromagnetic torque by the neural network are very accordant to the desired values as illustrated in figure (17 & 18).

5. The decoupling of the stator current components is exactly aligned in Neural-estimator strategy. The torque component (i_{qs}^*) is exactly analogues the electromagnetic torque (T_e) as shown in figure (19), and the flux component current (i_{ds}^*) is constant and exactly analogues the air-gap flux as shown in figure (20).

References:

- [1]Bimal K. Bose, "Modern Power Electronic and AC Drives", Prentice Hall, 2002.
- [2] Qusay L. Hamdi, "Design of Indirect Field-Oriented PWM Inverter for Three-Phase Induction Motor", Ph.D. Thesis, Al-Rasheed collage of engineering, University of Technology, 2007.
- [3]Yushaizad Yusof, Abdul Halim Mohd, "Simulation and Modeling of Stator Flux Estimator for Induction Motor Using Artificial Neural Network Technique", IEEE, 2003.
- [4]S.K. Pillai, "A First Course on Electrical Drives", second edition, 1989.
- [5]Fadhil A. Hassan, "Modeling And Implementation of SVPWM Driver of 3-Phase Induction Motor", Ms.c. thesis, University of Technology, Iraq, 2008.
- [6]Faa-Jeng Lin, Wen-Jyi Huang and Rong-Long Wai, "A Supervisory Fuzzy Neural Network Control System for Tracking Periodic Inputs", IEEE, Vol 7, February 1999.
- [7]Lina J. Rashad, "Excitation and Governing Control of a Power Generation Based Intelligent System", Ms.c. thesis, University of Technology, Iraq, 2008.

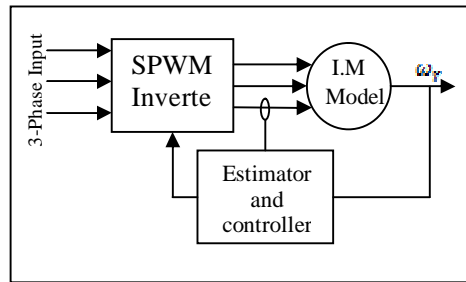


Figure (1) Block Diagram

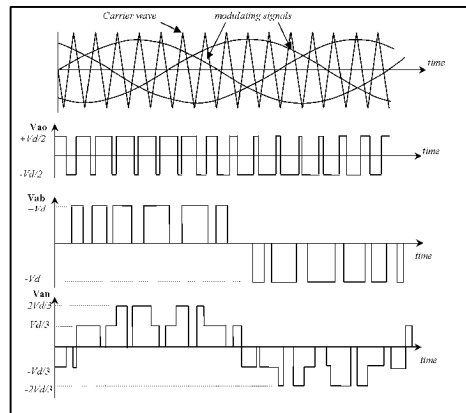


Figure (2) SPWM Principles

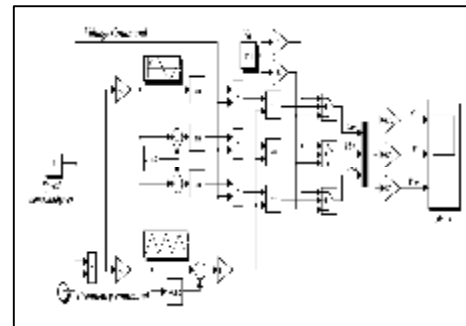


Figure (3) SPWM Simulation

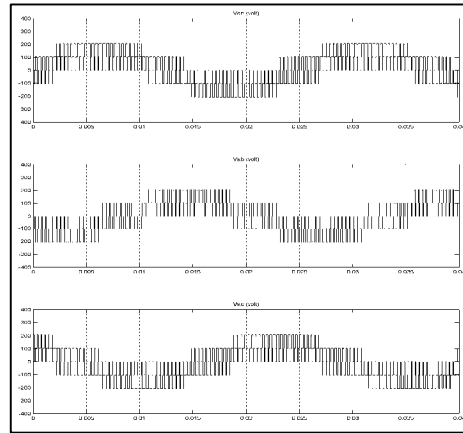


Figure (4) Linear Region Output Phase Voltage

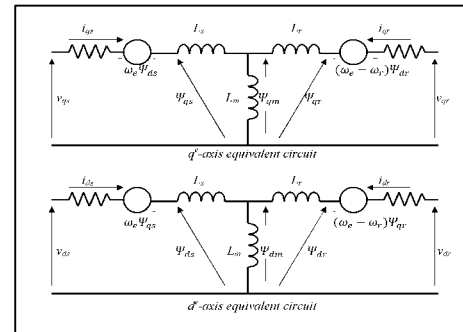


Figure (5) d^e-q^e I.M Equivalent Circuit

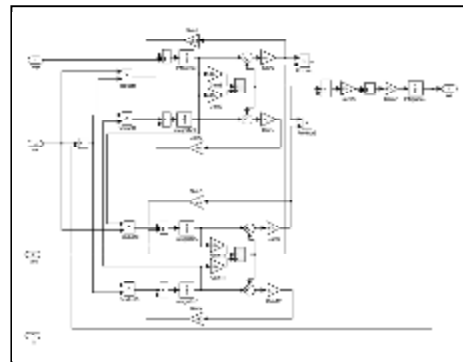


Figure (6) I.M Simulation

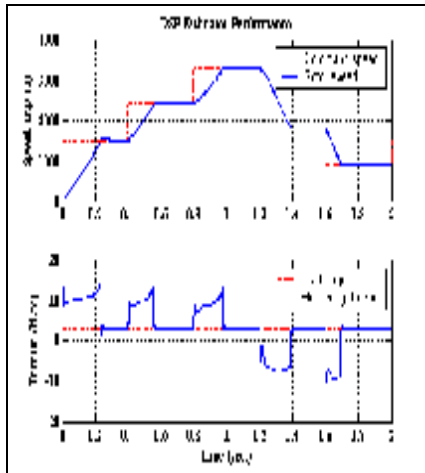


Figure (11) DSP System Performance

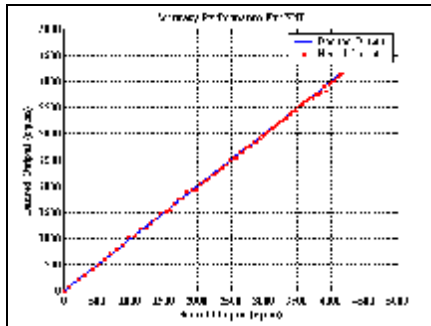


Figure (12-a) Accuracy Performance for Neural Network

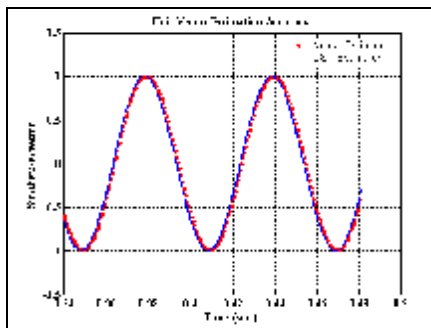


Figure (12-b) Unit Vector Estimation Accuracy

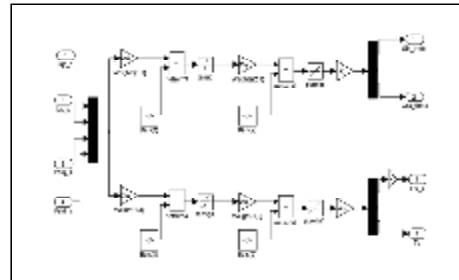


Figure (13) Neural Estimator Network Simulation

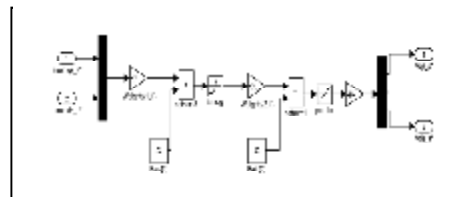


Figure (14) PI Neural-Based Controller Simulation

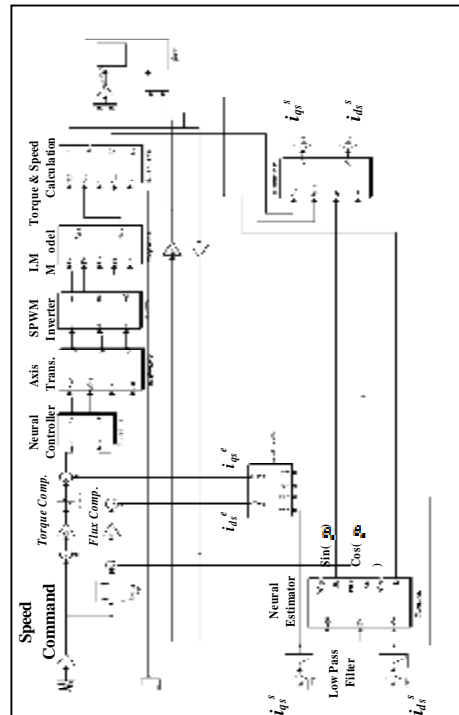


Figure (15) Overall Neural Estimator and Controller System Simulation

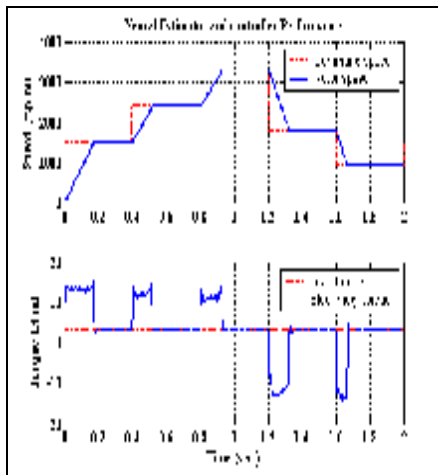


Figure (16) Neural System Performance

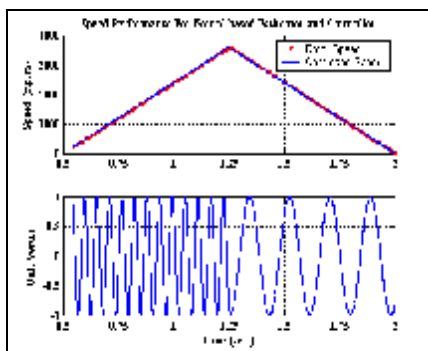


Figure (17) Speed & Unit Vector Accuracy Performances

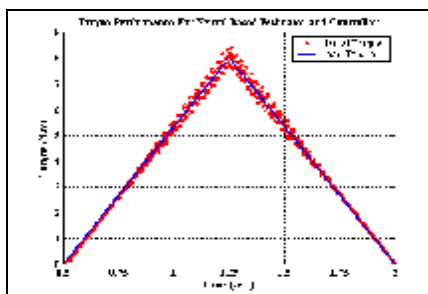


Figure (18) Torque Accuracy Performance

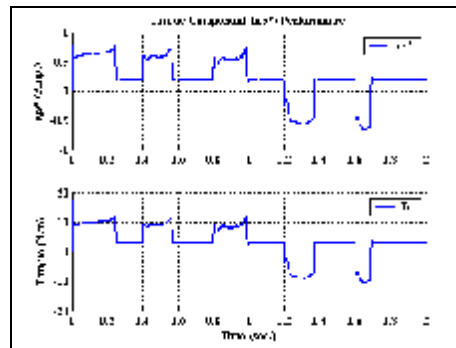


Figure (19) Torque & i_{ds}^* Current Component

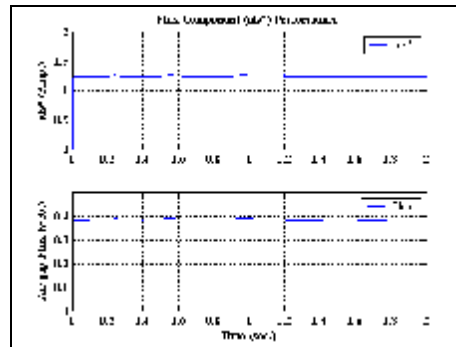


Figure (20) Flux & i_{ds}^* Current Component

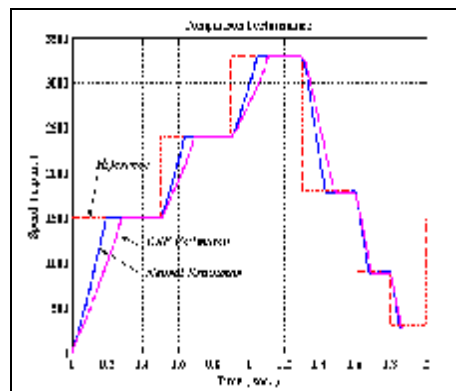


Figure (21) A Comparison Performance

Appendix:

The name plat of used I.M:
3-ph I.M, 380 v, 2.2 kw, 2 poles, 50
Hz, $L_s = 13.6$ mH, $L_r = 11.4$ mH,
 $R_s = 2.3$ Ω , $R_r = 3.4$ Ω , rotor inertia=
 $4.5 \cdot 10^{-3}$ kg/m².